Earth and Planetary Science Letters 525 (2019) 115737

Contents lists available at ScienceDirect

Earth and Planetary Science Letters

www.elsevier.com/locate/epsl

Hydroclimatic variability in Southeast Asia over the past two millennia

Jessica K. Wang [a], Kathleen R. Johnson [a,*], Andrea Borsato [b], Dillon J. Amaya [c], Michael L. Griffiths [d], Gideon M. Henderson [e], Silvia Frisia [b], Andrew Mason [e]

[a] Department of Earth System Science, University of California, Irvine, CA, 92697, USA
[b] School of Environmental and Life Sciences, University of Newcastle, NSW 2308, Australia
[c] Scripps Institution of Oceanography, University of California, San Diego, CA, 92093, USA
[d] Department of Environmental Science, William Paterson University, Wayne, NJ, 07470, USA
[e] Department of Earth Sciences, University of Oxford, South Parks Road, Oxford, OX1 3AN, UK

ARTICLE INFO

Article history:
Received 29 December 2018
Received in revised form 5 May 2019
Accepted 27 July 2019
Available online xxxx
Editor: I. Halevy

Keywords:
Asian monsoon
speleothem
paleoclimate
rainfall
solar forcing

ABSTRACT

The spatiotemporal variability of the Asian Monsoon (AM) over the last two millennia has been attributed to a combination of external solar and volcanic forcing and/or internal coupled atmosphere-ocean dynamics, but the relative importance of these mechanisms remains unresolved. The present knowledge of multidecadal to centennial-scale AM variability over Mainland Southeast Asia is not well-constrained, despite substantial progress in understanding seasonal to decadal variability from tree ring records. Here we present the first high-resolution stable isotope (δ^{13}C and δ^{18}O) speleothem record from northern Laos spanning the Common Era (~50 BCE to 1880 CE). The δ^{13}C record reveals substantial centennial-scale fluctuations primarily driven by local water balance. Notably, the driest period at our site occurred from ~1280 to 1430 CE, during the time of the Angkor droughts, supporting previous findings that this megadrought likely impacted much of Mainland Southeast Asia. In contrast, variations in stalagmite δ^{18}O reflect changes in rainfall upstream from our study site. Interestingly, the δ^{18}O record exhibits a positive correlation with solar activity that persists after 1200 CE, contrary to the findings in previous studies. Solar-forced climate model simulations reveal that these δ^{18}O variations may be driven by solar-forced changes in upstream rainout over the tropical Indian Ocean, which modify the δ^{18}O of moisture transported to our study site without necessarily affecting local rainfall amount. We conclude that future rainfall changes in Mainland Southeast Asia are likely to be superimposed on multidecadal to centennial-scale variations in background climate driven primarily by internal climate variability, whereas solar forcing may impact upstream rainout over the Indian Ocean.

© 2019 Elsevier B.V. All rights reserved.

1. Introduction

The Asian Monsoon (AM) system is known to vary on a range of timescales, from orbital to interannual (Berkelhammer et al., 2010; Cheng et al., 2016; Cook et al., 2010; Griffiths et al., 2016; Wang et al., 2005; Zhang et al., 2008). AM variability has been linked to orbitally-forced changes in Northern Hemisphere summer insolation (Cheng et al., 2016). Additionally, millennial-scale AM changes have been linked to North Atlantic ice rafting events and the corresponding changes in the strength of the Atlantic Meridional Overturning Circulation (AMOC) (Wang et al., 2001). However, there are fewer studies that have focused on the mechanisms underlying higher-frequency AM variability. Centennial to decadal-scale AM variations have thus far been attributed to some combination of external solar and volcanic forcing (Yan et al., 2015; Zhang et al., 2008) and/or internal coupled ocean-atmosphere dynamics (Berkelhammer et al., 2010; Buckley et al., 2010; Cook et al., 2010; Sinha et al., 2011a), but the relative importance of these mechanisms is still uncertain due, in part, to the paucity of sub-decadal resolution paleoclimate records. Furthermore, projections of future AM changes in response to anthropogenic greenhouse gas forcing are still a challenge for climate models (Mohtadi et al., 2016). While most models project that overall AM precipitation will increase despite a projected weakening of monsoon circulation, no such trends have been clearly observed (Christensen et al., 2013). Recent precipitation trends have instead exhibited substantial regional variability that has been primarily attributed to internal ocean-atmosphere dynamics (Conroy et al., 2011). Given the complex dynamic nature of the AM and the short length of instrumental observations, our understanding of regional AM variability remains incomplete. The development of robust and precisely

* Corresponding author.
E-mail address: kathleen.johnson@uci.edu (K.R. Johnson).

https://doi.org/10.1016/j.epsl.2019.115737
0012-821X/© 2019 Elsevier B.V. All rights reserved.

dated paleoclimate records is therefore critical to better characterize the timing and mechanisms of centennial to decadal-scale regional AM variability over the Common Era.

Speleothem oxygen isotope ($\delta^{18}O$) records from China and India have been widely utilized to reconstruct past AM variability (Cheng et al., 2016; Sinha et al., 2011a; Wang et al., 2001; Zhang et al., 2008), with more negative values widely interpreted as evidence for a stronger AM and vice-versa. However, the precise mechanism driving the $\delta^{18}O$ in the AM region is still debated and interpretations include changes in local or regional precipitation amount (Berkelhammer et al., 2010; Sinha et al., 2011a), precipitation seasonality (Wang et al., 2001), atmospheric circulation (Chiang et al., 2015; Zhang et al., 2018), and the degree of upstream rainout during transport (Pausata et al., 2011). While orbital and millennial scale $\delta^{18}O$ changes have been widely linked to changes in summer insolation and AMOC, respectively, several previous studies have suggested that decadal to centennial-scale speleothem $\delta^{18}O$ variability may be attributed to external solar changes due to significant spectral peaks at frequencies associated with known solar cycles (Neff et al., 2001; Zhang et al., 2008; Zhao et al., 2015). However, given the small radiative forcing associated with solar variability, the complex controls on speleothem $\delta^{18}O$, and the incomplete understanding of physical processes through which solar variations may influence the AM, the nature and robustness of the relationship remain unclear. Other speleothem $\delta^{18}O$ studies have attributed decadal to centennial-scale variability to internal coupled ocean-atmosphere modes, such as the El Niño Southern Oscillation (ENSO) and the Atlantic Multidecadal Oscillation (AMO) (Berkelhammer et al., 2010; Zhao et al., 2015). Few speleothem studies have utilized additional proxies, such as carbon isotopes, which when combined with $\delta^{18}O$ data could add valuable climate information to more fully examine the AM response to both internal climate variability and external forcings.

Speleothem carbon isotope variations ($\delta^{13}C$) have been found to reflect shifts in the local water balance through hydrologically-sensitive processes related to soil and vegetation efficiency and in or above-cave processes (Frisia et al., 2011; Genty et al., 2001; Johnson et al., 2006). Enhanced CO_2 degassing and calcite precipitation in the epikarst or on the cave ceiling during dry periods lead to preferential loss of $^{12}CO_2$ from the infiltrating water to the cave air, which shifts the $\delta^{13}C$ of subsequent stalagmite calcite to more positive values (Johnson et al., 2006). Similarly, decreased soil and root respiration during dry periods can contribute to lower soil pCO_2 and to more positive $\delta^{13}C$ values of the carbonate (Bajo et al., 2017). Despite the complex controls on speleothem carbon isotopes, shifts towards more positive $\delta^{13}C$ are often interpreted as drier conditions, whilst more negative $\delta^{13}C$ values are interpreted as wetter conditions above the cave site. For instance, a recent study from southern China reported that centennial-scale changes in speleothem $\delta^{13}C$ were sensitive to local water balance variations associated with regional hydrological change (Liu et al., 2016). Despite recent advances in understanding the factors that control speleothem $\delta^{13}C$ (Wong and Breecker, 2015), few studies from the AM region have focused on the link between speleothem $\delta^{13}C$ variability and local hydroclimate or monsoon variability.

At present, limited paleoclimate records that span the last two millennia exist across Mainland Southeast Asia (MSEA), where the majority of rainfall is delivered by the Southeast Asian Monsoon (Conroy et al., 2011). Even slight changes in the intensity or timing of monsoon rainfall can have profound societal and economic impacts on the region with recent severe droughts and floods (Thirumalai et al., 2017) highlighting the critical need to better constrain the nature of past and future hydroclimate changes. Tree rings and lake sediment records have provided insight on MSEA precipitation variability on interannual to centennial timescales (Buckley et al., 2010; Chawchai et al., 2015; Yamoah et al., 2016). Absolute-dated precipitation records from tree ring width series spanning the last several centuries have suggested that ENSO is one of the most important drivers for interannual to decadal-scale droughts in the region (Buckley et al., 2010; Cook et al., 2010). A multi-proxy record from lake sediments in northern Thailand has revealed multidecadal to centennial-scale precipitation variability during the last two millennia, which was linked to low-frequency ENSO-like patterns and/or shifts in the position of the intertropical convergence zone (ITCZ) (Chawchai et al., 2015; Yamoah et al., 2016). In contrast with several studies of speleothem $\delta^{18}O$ from the broader AM region (Zhang et al., 2008; Zhao et al., 2015), lake and tree ring records did not provide evidence for a strong solar variability influence on MSEA climate (Buckley et al., 2010). This disagreement between climate archives, along with the complex controls on precipitation $\delta^{18}O$, raises the possibility that solar activity may influence speleothem $\delta^{18}O$ variability without necessarily impacting local hydroclimate.

To address this issue, here we present the first high-resolution, precisely dated speleothem stable isotope ($\delta^{18}O$ and $\delta^{13}C$) record from MSEA spanning the last two millennia. The $\delta^{18}O$ and $\delta^{13}C$ records reveal substantial multidecadal to centennial-scale oscillations, which we interpret as reflecting variations in rainout upstream of our study site and local water balance, respectively. Our $\delta^{13}C$ results suggest that centennial-scale precipitation variations in the region are likely dominated by internal climate variability. Through comparisons with solar activity records and solar-forced climate model simulations, we propose that solar-forced changes in precipitation over the Indian Ocean may drive multidecadal to centennial-scale speleothem $\delta^{18}O$ variability at our site.

2. Study site and climatology

Tham Doun Mai Cave (TM cave; 20°45′N, 102°39′E) is a ~3,745 m-long cave located at 352 m above sea level in Luang Prabang Province, Laos (Fig. S1; Supplementary Material). Mean annual rainfall in the region is ~1,200 mm, ~70% of which is delivered during the summer monsoon season (June-September), when strong southwesterly winds transport warm moisture-laden air masses sourced primarily from the Indian Ocean and Bay of Bengal to MSEA (Fig. S1). Mean monthly rainfall $\delta^{18}O$ values exhibit strong seasonality, with the summer monsoon moisture being significantly depleted in ^{18}O with respect to boreal winter moisture.

Isotope-enabled climate model results showed that modern $\delta^{18}O$ of precipitation at TM cave is not significantly correlated to local precipitation amount (Yang et al., 2016). However, strong correlations with two measures of AM strength, sea level pressure and vertical wind shear over the Indian Ocean and Bay of Bengal, instead suggest an important influence of upstream rainout on precipitation $\delta^{18}O$ at TM cave (Yang et al., 2016). In this study, we utilize the term "AM intensity" to refer to the degree of rainout associated with this convective activity upstream from TM cave, which includes the Indian Ocean, Indian sub-continent, and the Bay of Bengal. Although the influence from the amount effect (i.e., a tendency for lower $\delta^{18}O$ values in rainfall from strongly convective systems) (Dansgaard, 1964) cannot be entirely ruled out, we interpret TM speleothem $\delta^{18}O$ values primarily as a proxy for AM intensity. Increased upstream rainout during strong AM periods leads to more negative $\delta^{18}O$ values at TM cave without necessarily requiring a change in local precipitation amount in northern Laos (Pausata et al., 2011).

3. Methods

3.1. Speleothem chronology

Speleothem TM-17 was sampled ~200 m from the cave entrance and was not actively growing at the time of collection. It

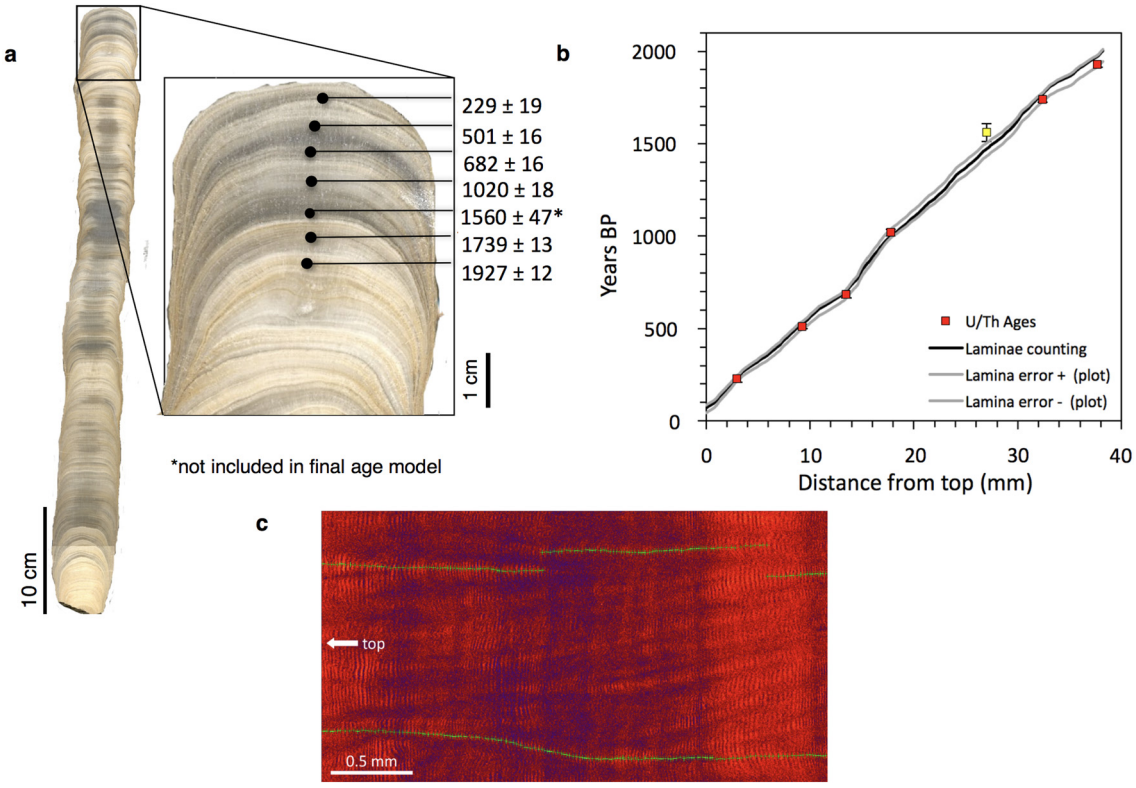

Fig. 1. TM-17 morphology and age model (a) Scanned image of stalagmite TM-17 cut parallel to the growth axis. Zoomed-in image shows the section of stalagmite TM-17 composed by alternating compact columnar calcite layers (dark grey) and porous columnar calcite layers. Black dots indicate the positions of ^{230}Th dates measured. The ages are reported in years BP (before 1950 CE). (b) Age-depth plot using the U–Th ages (red squares) coupled with the laminae counting. The 2σ U–Th error bars are shown, but in most cases are smaller than the symbols. The grey thick lines correspond to age model uncertainty constructed from the U–Th 2σ error bars by propagating the 3% laminae counting (LC) error within each section between two adjacent U–Th ages. The yellow square represents the U–Th age (U3) that was not included in the final age model due to the large uncertainty on the raw age, which indicates a poor analysis. (c) Strontium synchrotron micro XRF map of the central section of TM-17**.** The map is rendered in temperature scale (red = high, blue = low value). The alignments of green crosses centered on the lower intensities (blue) laminae at the top and bottom of the image visualize two sets of laminae counting.

is a 60 cm long, candle-shaped stalagmite, but for this study we focus only on the top ~4 cm. Seven powdered samples (~200 mg/each) were drilled from the central growth axis of TM-17 using a Dremel tool fitted with a diamond dental bur (Fig. 1a). ^{230}Th/^{234}U ages were determined using multi-collector inductively coupled plasma mass spectrometry (MC-ICP-MS) at the University of Oxford, UK (Table S1) following methods outlined in previous studies (Hu et al., 2008; Mason and Henderson, 2010). All samples were corrected for initial ^{230}Th using an initial ^{230}Th/^{232}Th value of 5.38 +5.38/−4.84 ppm. The U–Th ages lie in stratigraphic order and range from 229 ± 19 to 1927 ± 12 yr before present (years BP, where present equals 1950 CE), indicating an average growth rate of ~20 μm/yr (Fig. 1; Table S1). High-resolution analyses on TM-17 conducted via synchrotron radiation X-ray fluorescence (XRF) microscopy (Supplementary Materials) show clear laminations in Sr concentration spaced at ~20 μm intervals, suggesting that they are annual in nature. To further constrain the age model, we conducted annual laminae counting on the Sr synchrotron XRF map and anchored this floating laminae counting age model to the U–Th ages using a least-squares fit method (Domínguez-Villar et al., 2012) (Fig. 1c). The final age model indicates that TM-17 formed between ~50 BCE to 1880 CE with an average age uncertainty of 26 yr (Supplementary Material).

3.2. Stable isotope analyses

A total of 903 powdered samples were micromilled at 0.04 mm intervals (~2- to 4-yr resolution) along the central growth axis of TM-17. Powdered samples (~30-70 mg) were weighed and analyzed for carbon and oxygen isotope (δ^{13}C, δ^{18}O) composition on a Thermo Finnigan Kiel IV carbonate device coupled with a Delta V Plus isotope ratio mass spectrometer at the University of California, Irvine. All results are expressed using conventional δ notation in per mil (‰) relative to the V-PDB standard. A total of 18 standards (IAEA-CO-1, NBS-18, and OX, an in-house quality control standard) were analyzed during each run of 28 unknown samples. Duplicate measurements of NBS-18 and IAEA-CO-1 standards show a long-term standard deviation of 0.04‰ for δ^{13}C and 0.07‰ for δ^{18}O (1σ).

3.3. Model analyses

To assess the influence of solar-forced tropical climate variability on multidecadal TM-17 δ^{18}O fluctuations, we used runs from the Community Earth System Model Last Millennium Ensemble (CESM-LME) (Otto-Bliesner et al., 2016). CESM-LME is available from 850-2005 CE with a vertical resolution of 30 pressure levels in the atmosphere and a horizontal resolution of ~2° for the atmosphere and land and ~0.3°–1.0° for the ocean and sea ice coupled model. In the present study, we analyzed the ensemble mean of four runs forced only with varying solar intensity (Otto-Bliesner et al., 2016) and perturbed with slightly different initial conditions. To better compare our record with CESM-LME variables, we interpolated TM-17 δ^{18}O to regularly spaced time intervals of every two years from 50 BCE to 1878 CE (n = 965). Likewise, the ensemble mean anomalies were then annually averaged and interpolated to our regularly spaced age model from 850 CE to 1878 CE (n = 515). To isolate low-frequency variability, TM-17 δ^{18}O and model data were then subject to a 4th-order Butterworth filter with a 50-yr period cutoff. Comparisons were then

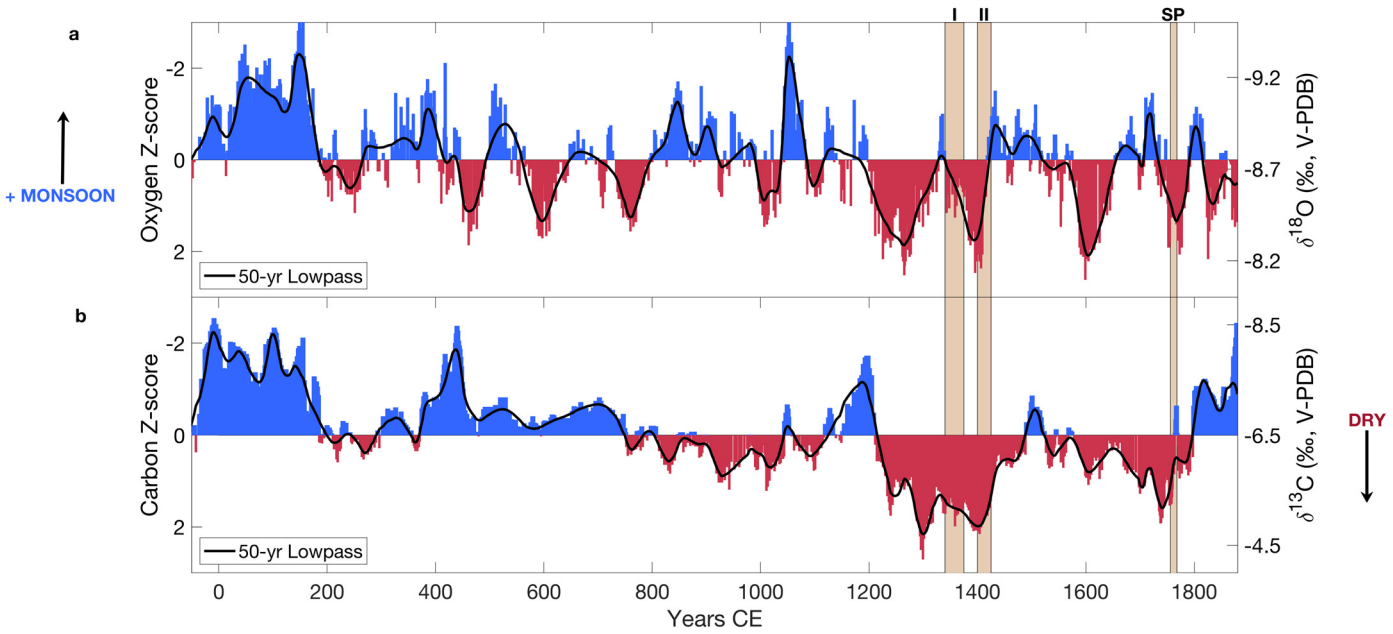

Fig. 2. Stable isotope record of Southeast Asian hydroclimate from stalagmite TM-17. (a) $\delta^{18}O$ record and (b) $\delta^{13}C$ record. Standard (z) scores are shown for records. The black lines represent the 50-yr low pass filtered data. $\delta^{18}O$ values are interpreted as reflecting monsoon intensity, whereby more negative z-scores (blue) reflect increased monsoon intensity (upstream rainout) and vice versa. $\delta^{13}C$ values are interpreted as a local water balance record, whereby more negative z-scores (blue) represent wetter conditions and positive values (red) represent drier conditions at the cave site. Vertical brown bars identify the Angkor I and II Droughts (I and II, respectively) (Buckley et al., 2010) and the Strange Parallels Drought (SP; 1756-1768 CE) (Cook et al., 2010).

made between our low-passed $\delta^{18}O$ record and the low-passed ensemble mean from 1200 CE to 1878 CE. We chose to focus on this time period due to the high temporal coherence multidecadal to centennial timescales between our record and the total solar intensity used to force CESM-LME that begins around 1200 CE (Fig. 3e, Figs. S5 and S6).

As a measure of the zonal circulation along the equator, we calculated the zonal mass streamfunction (ψ_x) as:

$$\psi_x(t, x, p) = \frac{2\pi a}{g} \int_0^p [u_D] dp \quad (1)$$

where a is the radius of the earth, g is the gravitational constant, p is pressure, and $[u_D]$ is the divergent component of the zonal wind field averaged from 5°S–5°N (Yu and Zwiers, 2010).

Correlation significance for the model analyses was determined using Monte-Carlo methods. First, we generated 1,000 different pairs of uncorrelated, white noise time series and subjected them to a 4th-order Butterworth filter with a 50-yr period cutoff. Then, we correlated these low-passed random pairs of time series and created a null distribution of correlation coefficients. Unless otherwise noted, correlations between TM-17 $\delta^{18}O$ and CESM-LME model data were taken to be significant if they fell outside of the 95% confidence interval of this null distribution.

4. Results

The TM-17 $\delta^{18}O$ values range from – 9.2‰ to – 8.0‰ and exhibit multidecadal to centennial-scale fluctuations with lower values recorded from ~50 BCE to 500 CE and higher values from 1200 CE to 1880 CE (Fig. 2a; Fig. S2). These variations are likely dominated by low-frequency changes in AM intensity, though they may also be modified in part by hydrological processes in the epikarst (Bradley et al., 2010; Evans et al., 2013) (Supplementary Material). These hydrologic effects have the potential to filter or reduce the amplitude of seasonal to interannual climate frequencies leading to hydrologic "smoothing" or reddening of the $\delta^{18}O$ signal during the proxy formation process as precipitation infiltrates through the epikarst. These processes therefore may shift interannual to decadal-scale speleothem $\delta^{18}O$ signals towards lower frequencies relative to the associated climate signals, though these effects are less likely to influence the multidecadal to centennial-scale variations we focus on here (Bradley et al., 2010; Dee et al., 2017; PAGES Hyro2k Consortium, 2017).

The TM-17 $\delta^{13}C$ values range from −8.4‰ to −4.4‰ and are characterized by multidecadal to centennial-scale variability that is superimposed on a millennium-long positive trend, with more negative values from ~50 BCE to 750 CE and more positive values from ~1200 to 1800 CE (Fig. 2b; Fig. S2). Considering that the TM-17 stalagmite has a regular and straight candle-shaped morphology and columnar fabric (Fig. 1), indicative of a slow and almost constant drip rate (Frisia and Borsato, 2010), it is reasonable to infer that the $\delta^{13}C$ increases were mainly driven by climate-related soil and/or vegetation processes associated with drier conditions (Mühlinghaus et al., 2007) (Supplementary Material). Similar to $\delta^{18}O$, it is also likely that vegetation and soil processes may act to smooth the interannual to decadal-scale precipitation variability, leading to apparent reddening of the $\delta^{13}C$ spectra compared with the precipitation signal.

5. Discussion

5.1. Regional monsoon variability and drought history

To evaluate the regional coherency of AM variability, we compare high-resolution, precisely dated speleothem records that span the last millennium or longer with the TM-17 $\delta^{18}O$ record. Stalagmite $\delta^{18}O$ records from Wanxiang and Dongge Caves, China (Zhang et al., 2008; Zhao et al., 2015) and a composite record from Dandak and Jhumar Caves, India (Sinha et al., 2011a, 2007) reveal similar multidecadal to centennial-scale $\delta^{18}O$ fluctuations over the last millennium, but the TM-17 record does not exhibit strong correlations with these records (Fig. 3). This disagreement may reflect a combination of chronological uncertainty, hydrologic processes, and/or differences in regional climatology and precipitation $\delta^{18}O$

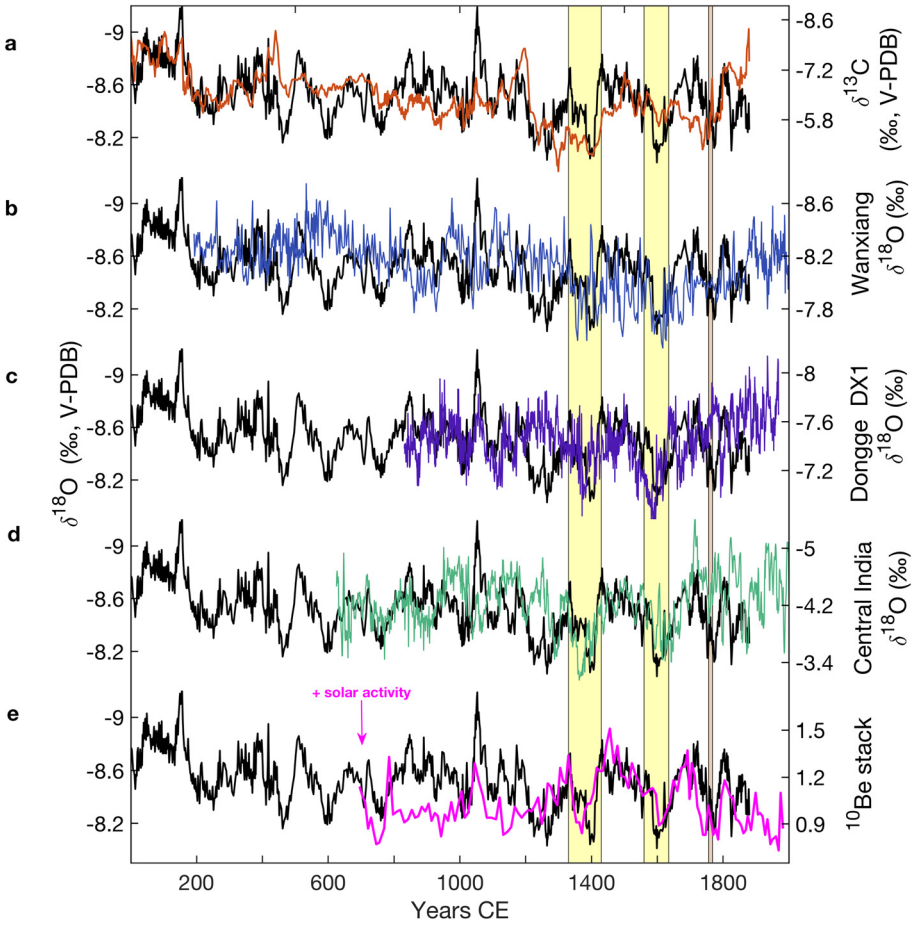

Fig. 3. Comparison of the TM-17 record with regional speleothem records and solar activity. The black line in all panels shows the stalagmite TM-17 $\delta^{18}O$ record compared with (a) Stalagmite TM-17 $\delta^{13}C$ (this study). (b) Stalagmite $\delta^{18}O$ from Wanxiang Cave, China (Zhang et al., 2008). (c) Stalagmite $\delta^{18}O$ from Dongge Cave, China (Zhao et al., 2015). (d) Composite stalagmite $\delta^{18}O$ record from Dandak and Jhumar Caves (Sinha et al., 2011a). (e) ^{10}Be stack derived from Central Antarctica ice cores (Delaygue and Bard, 2011). The vertical yellow bars denote the "weak monsoon" periods (1330-1430 CE and 1560-1635 CE). The y-axes in all panels are oriented such that weaker monsoon intensity and stronger solar activity are down.

controls (Hu et al., 2017; PAGES Hyro2k Consortium, 2017). Nevertheless, some common features of the records are worth discussing in more depth, such as two notable "weak monsoon" periods dated from 1330 to 1430 CE and from 1560 to 1635 CE that appear in all four records (Fig. 3). These periods correspond to the highest $\delta^{18}O$ values observed in the four stalagmite records and coincide with historical accounts of famine in India (Sinha et al., 2007) and social turmoil in China (Zhang et al., 2008). These weak monsoon periods recorded in these stalagmites suggest a common mechanism driving precipitation $\delta^{18}O$, which, as the modern precipitation $\delta^{18}O$ systematics suggests (Yang et al., 2016) does not necessarily imply synchronous precipitation amount changes at each site. For instance, decreased rainfall over the Indian monsoon region could lead to increased $\delta^{18}O$ at the Indian cave sites due to the amount effect, but also increased $\delta^{18}O$ of precipitation at "downstream" cave sites in Southeast and East Asia due to the upstream rainout mechanism and vice versa (Pausata et al., 2011). Alternatively, decreased rainout upstream of all sites could also lead to consistent shifts in $\delta^{18}O$ towards more positive values at each location.

The TM-17 $\delta^{13}C$ record exhibits the most positive values from 1280 to 1430 CE (Fig. 2b), suggesting the driest conditions of the last two millennia occurred during this period. Similarly, the Lake Pa Kho record from Thailand exhibits some of the driest conditions and lowest effective moisture from ~1300 to 1500 CE (Chawchai et al., 2015; Yamoah et al., 2016) (Fig. S3). Tree-ring based Palmer Drought Severity Index (PDSI) records from the AM region identified two major drought periods during the late 14th and early 15th centuries. These were referred to as the Angkor I and II droughts, which were then related to the collapse of the Khmer Empire (Buckley et al., 2014, 2010) (Fig. 3). This period also coincides with a growth hiatus in a ^{14}C-dated speleothem record from Cambodia, which was interpreted as indicating drought conditions (Hua et al., 2017). The tree ring records also highlight the spatially-extensive Strange Parallels (SP) megadrought (1756–1768 CE), which coincided with widespread famine in India and China (Buckley et al., 2014; Cook et al., 2010). This event is clearly expressed as positive $\delta^{13}C$ and $\delta^{18}O$ excursions in TM-17, indicating dry conditions in northern Laos and weakened monsoon intensity, respectively, at that time (Fig. 2).

Given the different controls on speleothem $\delta^{18}O$ and $\delta^{13}C$ values and the substantial variability in regional precipitation patterns in the AM region (Conroy et al., 2011), it is not unusual for regional proxy records to exhibit discrepancies or fall out of phase from one another during some periods. For example, the TM-17 $\delta^{13}C$ record, Vietnamese tree ring records (Buckley et al., 2010) and Thai lake records (Chawchai et al., 2015; Yamoah et al., 2016) do not show significant evidence for drought-like conditions during the second identified weak monsoon period from 1560 to 1635 CE (Fig. S3), which other studies identified as an extreme drought period in China and India (Zhang et al., 2008; Zhao et al., 2015). Furthermore, previous studies from the broader AM and tropical Pacific regions have focused on disentangling contrasting hypotheses to explain anomalous climate intervals, par-

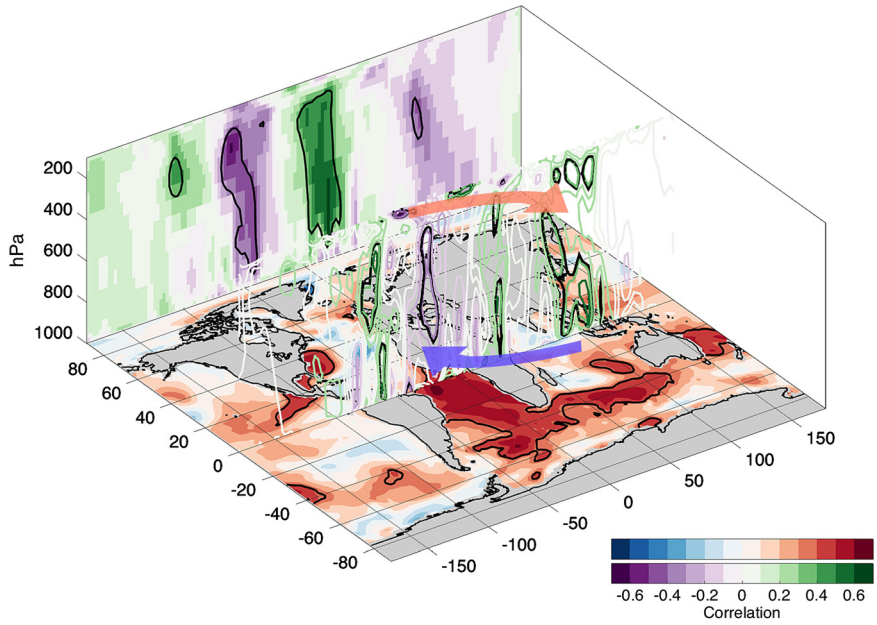

Fig. 4. Atmosphere-ocean response to solar forcing. TM-17 δ^{18}O correlations with ensemble mean CESM-LME solar forcing only SST anomalies (x/y plane shading), omega (ω) (x/z contours), and the zonal mass streamfunction (ψ) (x/z shading) averaged 5°S–5°N. The sign convention is such that positive (negative) ω and ψ correlations correspond to subsidence (convection) and clockwise (counter-clockwise) circulations, respectively. Note the ψ section on the back wall corresponds to values straddling the equator. Thick black contours indicate correlation significance at 95% confidence level. The blue arrow illustrates surface flow converging onto the warm tropical Atlantic, whereas the red arrow indicates upper-level divergence associated with the resulting deep convection.

ticularly the Medieval Climate Anomaly (MCA, 950-1250 CE) and the Little Ice Age (LIA, 1400-1850 CE) (Griffiths et al., 2016). Some paleoclimate proxy records link meridional shifts of the ITCZ to key changes in tropical Pacific hydroclimate (Sachs et al., 2009; Tierney et al., 2010; Zhang et al., 2008), while others implicate the influence of ENSO and associated zonal shifts of deep convection as the dominant drivers (Konecky et al., 2013; Yan et al., 2011). The TM-17 δ^{18}O record suggests decreased AM intensity, while the δ^{13}C record indicates overall drier conditions during the LIA, both of which are consistent with records of hydroclimatic variability in MSEA and Palau (Buckley et al., 2010; Richey and Sachs, 2016; Yamoah et al., 2016) (Fig. 2, Fig. S3). The drying trend and/or drought-like conditions observed from these records conflict with other paleoclimate records from the South China Sea (Yan et al., 2015) and Indonesia (Konecky et al., 2013), which show wetter conditions during the LIA that can be linked to a meridional ITCZ contraction and/or zonal deep convection shifts (Fig. S3). While the TM-17 record supports previous findings of dry conditions in MSEA during the LIA that point to a southward shift of the ITCZ or shifts in zonal convection, it has no clear evidence for a significant hydroclimatic shift during the MCA.

5.2. Solar influence on low-frequency δ^{18}O variability

Previous studies have suggested a relationship between solar activity and AM speleothem δ^{18}O changes on multidecadal to centennial timescales (Neff et al., 2001; Zhang et al., 2008; Zhao et al., 2015), though some found that the relationship was either temporally inconsistent or only played a minor role (Berkelhammer et al., 2010; Sinha et al., 2011b). We investigated the potential influence of solar activity by comparing the TM-17 δ^{18}O and δ^{13}C time series with three records of solar variability: total solar irradiance (TSI) (Vieira et al., 2011), sunspot number (Solanki et al., 2004), and ^{10}Be concentrations derived from ice cores (Delaygue and Bard, 2011) (Fig. 3e and Fig. S5). Reported correlation coefficients are Pearson's r values. Significance testing was conducted using a combination of 1,000 Monte Carlo iterations and time-series modeling in the frequency domain to consider the effect of serial correlation (Macias-Fauria et al., 2012). Notably, the most significant correlations between the δ^{18}O profile and reconstructed TSI ($r = 0.42$, $p < 0.01$), sunspot number ($r = 0.40$, $p < 0.05$), and ^{10}Be concentration ($r = -0.55$, $p < 0.01$) occur after 1200 CE for both unfiltered and 50-yr low passed filtered data (Figs. S5 and S6, Table S2). These significant correlations suggest decreased AM intensity corresponds with periods of increased solar irradiance and vice versa. By contrast, the TM-17 δ^{13}C record, exhibits no significant correlation with solar activity (Fig. S5), indicating that internal variability may be a more important driver of local precipitation on multidecadal to centennial timescales. We note that a potential caveat of this analysis stems from the age uncertainty in the proxy records (Hu et al., 2017), but given the strong similarities between the TM-17 δ^{18}O record and all three solar proxy records on multidecadal to centennial timescales, this relationship is worth further consideration. We therefore focus the remainder of our discussion on the potential solar influence on the TM-17 δ^{18}O record, which does appear to be consistent with changes in solar irradiance (Figs. S5 and S6).

To further investigate solar influence, we conducted cross-wavelet analyses between the δ^{18}O values and solar activity proxy records (Fig. S6). A strong shared power on multidecadal to centennial timescales between δ^{18}O and TSI, sunspot number, and ^{10}Be was observed. While the phasing between δ^{18}O and sunspot number oscillates, suggesting a less consistent influence of solar irradiance, there is consistent phasing post-1200 CE among all three solar proxies, specifically during the Spörer (1400-1510 CE) and Maunder (1645-1715 CE) Minimums (Figs. S5 and S6). Spectral analysis of the TM-17 δ^{18}O data does not provide evidence for a robust or persistent ~210 yr cycle (Fig. S2 and Supplementary Material), whereas other stalagmite records have revealed significant periodicities similar to the ~210-year solar cycle of de Vries-Suess (Novello et al., 2016; Wang et al., 2005). Persistent multidecadal to centennial-scale periodicities, however, emerge in the wavelet transform analysis (Fig. S2) as well as persistent centennial-scale power at in the wavelet coherence analysis with the solar proxies (Fig. S6), in particular after 1200 CE.

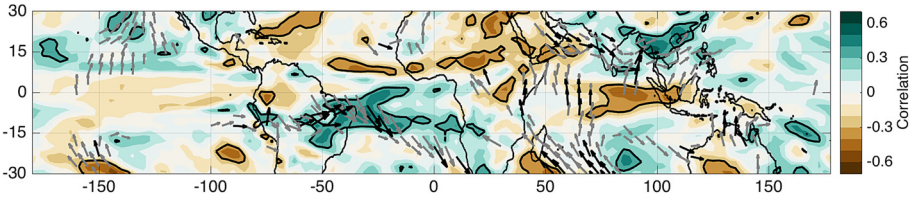

Fig. 5. TM-17 δ^{18}O correlated with ensemble mean CESM-LME solar forcing-only precipitation. TM-17 δ^{18}O correlated with CESM-LME total precipitation rate (shading) and 850 mb wind fields (arrows). Thick black contours and black (grey) arrows indicate correlation significance at 95% (80%) confidence level based on the distribution of 1,000 randomly generated low-pass filtered time series. All time series were subjected to a 50-year low pass filter.

This monsoon-solar relationship observed in our record contrasts with earlier studies that observed the opposite relationship, such that periods of increased AM rainfall correspond with periods of increased solar irradiance (Zhang et al., 2008; Zhao et al., 2015). While these Chinese stalagmite studies note that some periods of decreased solar irradiance, such as the Spörer Minimum (1400-1510 CE), coincide with wetter conditions, they attribute this to the influence of internal climate variability (Zhang et al., 2008; Zhao et al., 2015). A recent southeastern Tibetan Plateau stalagmite δ^{18}O record, on the other hand, revealed a monsoon-solar relationship similar to our findings: multiple periods of increased AM rainfall (more negative δ^{18}O) were associated with decreased solar activity over the last millennium (Tan et al., 2018). Similarly, a positive relationship between South American Summer Monsoon (SASM) intensity and solar irradiance on centennial timescales was recently inferred from a stalagmite δ^{18}O record from Midwestern Brazil (Novello et al., 2016). This suggests that solar forcing could potentially lead to an anti-phase relationship between SASM and AM speleothem records, similar to the so-called global monsoon pattern observed on longer timescales and linked with meridional ITCZ shifts (Cheng et al., 2012). A comparison between our TM-17 δ^{18}O record and SASM proxy records, however, does not show a significant inverse relationship on multidecadal to centennial timescales (Fig. S4). This mismatch may reflect multiple factors, including chronological limitations, regional variability in monsoon precipitation patterns, differing controls on speleothem δ^{18}O, and/or the complex climate dynamics linking AM with SASM climate.

In addition to an opposite monsoon-solar relationship, the temporal nature of the relationship also differs between our study and previously published records, all of which suggest non-stationary behavior in the solar forcing-AM relationship. For example, the Wanxiang Cave record showed similar timing between AM and solar irradiance peaks between ~950–1250 CE (Zhang et al., 2008), whereas the Dandak Cave record showed coherence between Indian summer monsoon precipitation amount and solar variability from ~800–1290 CE (Berkelhammer et al., 2010). As a result of these temporally inconsistent relationships, both studies concluded that internal climate variability was likely a more important factor driving local hydroclimate change. It is interesting that our observed monsoon-solar relationship appears to strengthen at ~1200 CE, around the time these other relationships weakened, and persists for the remainder of the record (~680-year period). This may reflect true spatiotemporal variability in the response of precipitation δ^{18}O to solar forcing in the AM region (Tan et al., 2018), though could also reflect the variable influence of internal coupled climate modes such as ENSO or the AMO on AM intensity (Zhao et al., 2015; Berkelhammer et al., 2010).

Overall, our results imply that solar variability may exhibit a significant influence on the TM δ^{18}O record, in particular since 1200 CE. These results warrant further consideration for the role of solar forcing on changes in AM precipitation and, hence speleothem, δ^{18}O. Here we conduct a more through exploration of the potential mechanisms underlying the observed strong positive correlation between TM-17 δ^{18}O and solar variability (Fig. 3e, Figs. S5 and S6) utilizing climate model simulations.

5.3. Atlantic SSTs influence Asian monsoon precipitation $\delta^{18}O$

To explore solar-forced mechanisms that could influence low-frequency δ^{18}O variability at our site, we correlated the low-pass filtered TM-17 δ^{18}O record (50-year cutoff) with the ensemble mean of the "solar forcing only" simulations in the Community Earth System Model Last Millennium Ensemble (CESM-LME) (Otto-Bliesner et al., 2016). Each solar-forced ensemble member of CESM-LME is initialized by slightly different initial conditions, which largely cancel out in the ensemble mean. Therefore, CESM-LME ensemble mean variability can be interpreted as having been driven by the common external forcing (i.e. solar forcing). Since TM-17 δ^{18}O showed some consistency with the same solar variability that is used to force CESM-LME, it is reasonable to compare our time series directly to the CESM-LME ensemble mean as a first approximation of how solar forcing may influence AM intensity as it pertains to the time variability of our record.

We primarily focused on the period since 1200 CE, since TM-17 δ^{18}O exhibits significant correlations during this time period with all three solar records (Table S2). Correlations of TM-17 δ^{18}O with solar-forced CESM-LME sea surface temperature (SST) anomalies reveal the strongest and most significant positive correlations with tropical Atlantic SSTs (Fig. 4). This relationship is significant in all four solar-forced ensemble members (Fig. S7), increasing our confidence that these correlations are not spurious. In addition, we repeated the model analysis for the full overlapping period between the δ^{18}O and LME runs in the solar-only forcing runs. The results are qualitatively consistent, suggesting that the relationship is physically consistent (Fig. S8).

Previous studies have suggested that the relatively small radiative forcing from solar variability could potentially explain large SST changes in the Atlantic via non-linear responses of the climate system to amplifying feedbacks (Gray et al., 2010). For instance, a "top-down" mechanism was proposed, wherein solar-induced changes to stratospheric ozone and temperature gradients propagate downwards to influence North Atlantic atmospheric and ocean circulation (Meehl et al., 2009). These changes may be further amplified through feedbacks related to the AMOC (Caesar et al., 2018). Alternatively, it has been proposed that the small solar forcing signal may be amplified through "bottom-up" processes involving coupled atmosphere-ocean dynamics and associated changes to the Walker and Hadley circulation (Meehl et al., 2009). Regardless of how tropical Atlantic SSTs may respond to solar forcing, we utilized the CESM-LME solar-forced simulation to further explore mechanisms through which solar-forced SST changes in the tropical Atlantic could influence AM intensity and, hence, speleothem δ^{18}O at the TM cave site.

Our results show that δ^{18}O is significantly negatively correlated with a dipole of zonal mass streamfunction (ψ_x) circulation anomalies that straddle the tropical Atlantic and are consistent with the low-level convergence of near-surface winds initiated by

warmer Atlantic SSTs (Fig. 4 back wall shading). These convergences lead to increased deep convection over the tropical Atlantic, which is also apparent in $\delta^{18}O$ correlations with model vertical velocity (ω) (Fig. 4 equatorial vertical cross-section). Deep convection over the warm Atlantic is compensated by broad zonal bands of atmospheric subsidence over much of eastern Africa and the eastern tropical Indian Ocean, as indicated by positive correlations between CESM-LME ω and TM-17 $\delta^{18}O$ over these regions (Fig. 4). Subsidence over the tropical Indian Ocean consequently promotes increased atmospheric stability, lower cloud heights, and decreased precipitation, which are consistent with correlations between speleothem $\delta^{18}O$ values correlations and modeled precipitation (Fig. 5). Taken together, our results suggest that less upstream rainout over the tropical Indian Ocean, a key source of moisture to the broad AM region (Baker et al., 2015; Pathak et al., 2017), could lead to more positive $\delta^{18}O$ values of the water vapor reaching TM. Correlations between TM-17 $\delta^{18}O$ with 850 mb winds reveal increased cross-equatorial southerly winds from the tropical Indian Ocean and further supports that decreased precipitation over the tropical Indian Ocean could lead to the transport of higher $\delta^{18}O$ moisture to TM Cave (Fig. 4). These changes may be further reinforced by increased contribution of ^{18}O enriched moisture from the Bay of Bengal. However, it is difficult to quantitatively distinguish the relative importance of upstream rainout or other potential factors (such as moisture source region or rainfall amount) controlling multidecadal to centennial-scale $\delta^{18}O$ variability without long-term isotope-enabled climate model simulations and other multi-proxy speleothem data.

Finally, we note that volcanic eruptions represent the largest natural forcing to the climate system over the last millennium (Robock, 2000) and can potentially explain long-term trends seen in last millennium reconstructions (McGregor et al., 2015). To investigate whether volcanic forcing could provide an alternate explanation for the TM-17 $\delta^{18}O$ variability, we repeated our analyses with the CESM LME volcanic-only runs and found no similar correlations that would indicate a substantial volcanic influence on our record (not shown), which provides us confidence in our solar results. However, when we repeated our analyses using the CESM full-forcing runs, we found that the full forcing results were more similar to the volcanic-only runs. A possible explanation may be that strong volcanic forcing events are the single largest radiative forcing agents in the fully forced ensemble mean and therefore dominate the overall signal (Otto-Bliesner et al., 2016). As such, this may make it difficult to identify solar-forced changes in the full-forcing experiments that are relatively subtle compared to the strong volcanic eruptions used to force CESM-LME. Additionally, we note the large uncertainties in the timing and magnitude of volcanic eruptions used to force CESM-LME (Sigl et al., 2014). Finally, we note that our record does not preclude the possibility of volcanic influence on interannual to decadal-scale precipitation $\delta^{18}O$ variability, which may be reddened or otherwise obscured by karst hydrologic processes. Therefore, despite these discrepancies, our results may still offer insight on the influence of solar forcing on multi-decadal to centennial-scale precipitation $\delta^{18}O$ variability.

6. Conclusions

This study presents a new high-resolution speleothem stable isotope ($\delta^{18}O$ and $\delta^{13}C$) record from northern Laos that spans most of the Common Era (~50 BCE to 1880 CE). The $\delta^{18}O$ record is interpreted to reflect upstream rainout over the Indian Ocean, Bay of Bengal, and Indian monsoon region, whereas the $\delta^{13}C$ record reflects local water balance through impacts on soil-vegetation processes. The $\delta^{18}O$ record contains significant multidecadal to centennial-scale variability and exhibits positive correlations with records of solar variability, which are opposite to those previously reported (Zhang et al., 2008; Zhao et al., 2015). The $\delta^{13}C$ record, on the other hand, shows no relationship to solar forcing, but does contain significant centennial-scale variability, with generally dry conditions throughout the LIA. The driest conditions of the record occur during the 13th-15th centuries, consistent with other regional records (Buckley et al., 2014, 2010; Chawchai et al., 2015; Yamoah et al., 2016). Overall, the $\delta^{13}C$ record provides evidence that internal variability likely played a more important role than solar forcing in driving multidecadal to centennial-scale precipitation variability in MSEA.

Based on the observed solar forcing-$\delta^{18}O$ relationship, this study proposes one hypothesis to explain multidecadal to centennial-scale variations in speleothem $\delta^{18}O$ possibly associated with solar-forced increases in convection and rainfall over the Indian Ocean. Results of the solar forcing only experiments from the CESM-LME suggest that increased tropical Atlantic SSTs resulting from increased solar irradiance may lead to modifications in zonal atmospheric circulation and increased subsidence over the tropical Indian Ocean, leading to less upstream rainout over a key moisture source for the AM region (Baker et al., 2015; Pathak et al., 2017). This proposed mechanism offers a plausible explanation for the increased speleothem $\delta^{18}O$ values at our site during periods of increased solar activity, without requiring any solar-forced changes in local precipitation amount, thus providing a potential explanation for some periods when the $\delta^{18}O$ and $\delta^{13}C$ records differ.

While age uncertainty and proxy formation processes present challenges for conducting this type of multi-proxy analysis and data-model comparison (Hu et al., 2017; PAGES Hyro2k Consortium, 2017), the data presented here provide a baseline of MSEA natural climate variability on multidecadal to centennial timescales, which is critical for understanding the extent that external forcing and internal variability will impact AM intensity and MSEA water resources in the coming decades. Through a novel model-data comparison, we propose a new mechanism to potentially explain solar influence on AM region precipitation $\delta^{18}O$. Future research including development of additional high-resolution paleoclimate records, isotope-enabled climate model analyses, and proxy system modeling will be needed to further constrain the impacts of external forcing and internal climate variability on speleothem $\delta^{18}O$ and $\delta^{13}C$ records in the AM region.

Data archiving

The speleothem data reported here are archived at the NOAA National Centers for Environmental Information's World Data Service for Paleoclimatology.

Acknowledgements

We thank Joyce White, Bounheuang Bouasisengpaseuth, Norseng Sayvongdouane, Sengphone Keophanhya and other participants in the Middle Mekong Archaeology Project and Lao government officials and departments for their assistance with the fieldwork, which was funded in part by Henry Luce Foundation grant to the University of Pennsylvania Museum. We would like to thank D. Zhang for assistance with stable isotope analyses and D. Howard, V. Vanghi, and E. Anderson for assistance in synchrotron analyses. This work was supported by National Science Foundation P2C2 awards 1603056 and 1405472 to K.R.J., and National Science Foundation awards 1602947 and 1404932 and a William Paterson University Center for Research summer grant to M.L.G. This work was also supported by National Science Foundation Graduate Research Fellowships DGE-1321846 to J.K.W and DGE-1144086

to D.J.A. Petrographic and synchrotron work was supported by the Australian Research Council Discovery Project grant DP160101058 to S.F. The XRF analyses were undertaken at the X-ray fluorescence microscopy beamline of the Australian Synchrotron, Victoria, Australia.

Appendix A. Supplementary material

Supplementary material related to this article can be found online at https://doi.org/10.1016/j.epsl.2019.115737.

References

Bajo, P., Borsato, A., Drysdale, R., Hua, Q., Frisia, S., Zanchetta, G., Hellstrom, J., Woodhead, J., 2017. Stalagmite carbon isotopes and dead carbon proportion (DCP) in a near-closed-system situation: an interplay between sulphuric and carbonic acid dissolution. Geochim. Cosmochim. Acta 210, 208–227. https://doi.org/10.1016/J.GCA.2017.04.038.

Baker, A.J., Sodemann, H., Baldini, J.U.L., Breitenbach, S.F.M., Johnson, K.R., van Hunen, J., Pingzhong, Z., 2015. Seasonality of westerly moisture transport in the East Asian summer monsoon and its implications for interpreting precipitation δ^{18}O. J. Geophys. Res. 120, 5850–5862. https://doi.org/10.1002/2014JD022919.

Berkelhammer, M., Sinha, A., Mudelsee, M., Cheng, H., Edwards, R.L., Cannariato, K., 2010. Persistent multidecadal power of the Indian Summer Monsoon. Earth Planet. Sci. Lett. 290, 166–172. https://doi.org/10.1016/j.epsl.2009.12.017.

Bradley, C., Baker, A., Jex, C.N., Leng, M.J., 2010. Hydrological uncertainties in the modelling of cave drip-water δ^{18}O and the implications for stalagmite palaeoclimate reconstructions. Quat. Sci. Rev. 29, 2201–2214. https://doi.org/10.1016/j.quascirev.2010.05.017.

Buckley, B.M., Anchukaitis, K.J., Penny, D., Fletcher, R., Cook, E.R., Sano, M., Nam, L.C., Wichienkeeo, A., Minh, T.T., Hong, T.M., 2010. Climate as a contributing factor in the demise of Angkor, Cambodia. Proc. Natl. Acad. Sci. USA 107, 6748–6752. https://doi.org/10.1073/pnas.0910827107.

Buckley, B.M., Fletcher, R., Yu Simon Wang, S., Zottoli, B., Pottier, C., 2014. Monsoon extremes and society over the past millennium on mainland Southeast Asia. Quat. Sci. Rev. 95, 1–19. https://doi.org/10.1016/j.quascirev.2014.04.022.

Caesar, L., Rahmstorf, S., Robinson, A., Feulner, G., Saba, V., 2018. Observed fingerprint of a weakening Atlantic Ocean overturning circulation. Nature 556, 191–196. https://doi.org/10.1038/s41586-018-0006-5.

Chawchai, S., Chabangborn, A., Fritz, S., Väliranta, M., Mörth, C.-M., Blaauw, M., Reimer, P.J., Krusic, P.J., Löwemark, L., Wohlfarth, B., 2015. Hydroclimatic shifts in northeast Thailand during the last two millennia – the record of Lake Pa Kho. Quat. Sci. Rev. 111, 62–71. https://doi.org/10.1016/j.quascirev.2015.01.007.

Cheng, H., Edwards, R.L., Sinha, A., Spötl, C., Yi, L., Chen, S., Kelly, M., Kathayat, G., Wang, X., Li, X., Kong, X., Wang, Y., Ning, Y., Zhang, H., 2016. The Asian monsoon over the past 640,000 years and ice age terminations. Nature 534, 640–646. https://doi.org/10.1038/nature18591.

Cheng, H., Sinha, A., Wang, X., Cruz, F.W., Edwards, R.L., 2012. The Global Paleomonsoon as seen through speleothem records from Asia and the Americas. Clim. Dyn. 39, 1045–1062. https://doi.org/10.1007/s00382-012-1363-7.

Chiang, J.C.H., Fung, I.Y., Wu, C.-H., Cai, Y., Edman, J.P., Liu, Y., Day, J.A., Bhattacharya, T., Mondal, Y., Labrousse, C.A., 2015. Role of seasonal transitions and westerly jets in East Asian paleoclimate. Quat. Sci. Rev. 108, 111–129. https://doi.org/10.1016/J.QUASCIREV.2014.11.009.

Christensen, J.H., Kumar, K.K., Aldrian, E., An, S.-I., Cavalcanti, I.F.A., Castro, M., de Dong, W., Goswami, P., Hall, A., Kanyanga, J.K., Kitoh, A., Kossin, J., Lau, N.-C., Renwick, J., Stephenson, D.B., Xie, S.P., Zhou, T., 2013. Climate phenomena and their relevance for future regional climate change. In: Climate Change 2013: The Physical Science Basis, Contribution of Working Group I to the Fifth Assessment Report of the Intergovernmental Panel on Climate Change. Cambridge University Press, Cambridge, UK, New York, USA, pp. 1217–1308.

Conroy, J.L., Overpeck, J.T., Conroy, J.L., Overpeck, J.T., 2011. Regionalization of present-day precipitation in the greater monsoon region of Asia. J. Clim. 24, 4073–4095. https://doi.org/10.1175/2011JCLI4033.1.

Cook, E.R., Anchukaitis, K.J., Buckley, B.M., D'Arrigo, R.D., Jacoby, G.C., Wright, W.E., 2010. Asian monsoon failure and megadrought during the last millennium. Science 328, 486–489.

Dansgaard, W., 1964. Stable isotopes in precipitation. Tellus 16, 436–468. https://doi.org/10.1111/j.2153-3490.1964.tb00181.x.

Dee, S.G., Parsons, L.A., Loope, G.R., Overpeck, J.T., Ault, T.R., Emile-Geay, J., 2017. Improved spectral comparisons of paleoclimate models and observations via proxy system modeling: implications for multi-decadal variability. Earth Planet. Sci. Lett. 476, 34–46. https://doi.org/10.1016/J.EPSL.2017.07.036.

Delaygue, G., Bard, E., 2011. An Antarctic view of Beryllium-10 and solar activity for the past millennium. Clim. Dyn. 36, 2201–2218. https://doi.org/10.1007/s00382-010-0795-1.

Domínguez-Villar, D., Baker, A., Fairchild, I.J., Edwards, R.L., 2012. A method to anchor floating chronologies in annually laminated speleothems with U–Th dates. Quat. Geochronol. 14, 57–66. https://doi.org/10.1016/J.QUAGEO.2012.04.019.

Evans, M.N., Tolwinski-Ward, S.E., Thompson, D.M., Anchukaitis, K.J., 2013. Applications of proxy system modeling in high resolution paleoclimatology. Quat. Sci. Rev. 76, 16–28. https://doi.org/10.1016/j.quascirev.2013.05.024.

Frisia, S., Borsato, A., 2010. Chapter 6: Karst. In: Developments in Sedimentology, vol. 61, pp. 269–318.

Frisia, S., Fairchild, I.J., Fohlmeister, J., Miorandi, R., Spötl, C., Borsato, A., 2011. Carbon mass-balance modelling and carbon isotope exchange processes in dynamic caves. Geochim. Cosmochim. Acta 75, 380–400. https://doi.org/10.1016/j.gca.2010.10.021.

Genty, D., Baker, A., Massault, M., Proctor, C., Gilmour, M., Pons-Branchu, E., Hamelin, B., 2001. Dead carbon in stalagmites: carbonate bedrock paleodissolution vs. ageing of soil organic matter: implications for ^{13}C variations in speleothems. Geochim. Cosmochim. Acta 65, 3443–3457. https://doi.org/10.1016/S0016-7037(01)00697-4.

Gray, L.J., Beer, J., Geller, M., Haigh, J.D., Lockwood, M., Matthes, K., Cubasch, U., Fleitmann, D., Harrison, G., Hood, L., Luterbacher, J., Meehl, G.A., Shindell, D., van Geel, B., White, W., 2010. Solar influences on climate. Rev. Geophys. 48, RG4001. https://doi.org/10.1029/2009RG000282.

Griffiths, M.L., Kimbrough, A.K., Gagan, M.K., Drysdale, R.N., Cole, J.E., Johnson, K.R., Zhao, J.-X., Cook, B.I., Hellstrom, J.C., Hantoro, W.S., 2016. Western Pacific hydroclimate linked to global climate variability over the past two millennia. Nat. Commun. 7, 11719. https://doi.org/10.1038/ncomms11719.

Hu, C., Henderson, G.M., Huang, J., Xie, S., Sun, Y., Johnson, K.R., 2008. Quantification of Holocene Asian monsoon rainfall from spatially separated cave records. Earth Planet. Sci. Lett. 266, 221–232. https://doi.org/10.1016/J.EPSL.2007.10.015.

Hu, J., Emile-Geay, J., Partin, J., 2017. Correlation-based interpretations of paleoclimate data – where statistics meet past climates. Earth Planet. Sci. Lett. 459, 362–371. https://doi.org/10.1016/J.EPSL.2016.11.048.

Hua, Q., Cook, D., Fohlmeister, J., Penny, D., Bishop, P., Buckman, S., 2017. Radiocarbon dating of speleothem record of paleoclimate for Angkor, Cambodia. https://doi.org/10.1017/RDC.2017.115.

Johnson, K.R., Hu, C., Belshaw, N.S., Henderson, G.M., 2006. Seasonal trace-element and stable-isotope variations in a Chinese speleothem: the potential for high-resolution paleomonsoon reconstruction. Earth Planet. Sci. Lett. 244, 394–407. https://doi.org/10.1016/j.epsl.2006.01.064.

Konecky, B.L., Russell, J.M., Rodysill, J.R., Vuille, M., Bijaksana, S., Huang, Y., 2013. Intensification of southwestern Indonesian rainfall over the past millennium. Geophys. Res. Lett. 40, 386–391. https://doi.org/10.1029/2012GL054331.

Liu, D., Wang, Y., Cheng, H., Lawrence Edwards, R., Kong, X., Li, T.-Y., 2016. Strong coupling of centennial-scale changes of Asian monsoon and soil processes derived from stalagmite δ^{18}O and δ^{13}C records, southern China. https://doi.org/10.1016/j.yqres.2016.02.008.

Macias-Fauria, M., Grinsted, A., Holopainen, J., 2012. Persistence matters: estimation of the statistical significance of paleoclimatic reconstruction statistics from autocorrelated time series. Dendrochronologia 30, 179–187. https://doi.org/10.1016/J.DENDRO.2011.08.003.

Mason, A.J., Henderson, G.M., 2010. Correction of multi-collector-ICP-MS instrumental biases in high-precision uranium-thorium chronology. Int. J. Mass Spectrom. 295, 26–35. https://doi.org/10.1016/j.ijms.2010.06.016.

McGregor, H.V., Evans, M.N., Goosse, H., Leduc, G., Martrat, B., Addison, J.A., Mortyn, P.G., Oppo, D.W., Seidenkrantz, M.-S., Sicre, M.-A., Phipps, S.J., Selvaraj, K., Thirumalai, K., Filipsson, H.L., Ersek, V., 2015. Robust global ocean cooling trend for the pre-industrial Common Era. Nat. Geosci. 8, 671–677. https://doi.org/10.1038/ngeo2510.

Meehl, G.A., Arblaster, J.M., Matthes, K., Sassi, F., van Loon, H., 2009. Amplifying the Pacific climate system response to a small 11-year solar cycle forcing. Science 325, 1114–1118. https://doi.org/10.1126/science.1172872.

Mohtadi, M., Prange, M., Steinke, S., 2016. Palaeoclimatic insights into forcing and response of monsoon rainfall. Nature 533, 191–199. https://doi.org/10.1038/nature17450.

Mühlinghaus, C., Scholz, D., Mangini, A., 2007. Modelling stalagmite growth and δ^{13}C as a function of drip interval and temperature. Geochim. Cosmochim. Acta 71, 2780–2790. https://doi.org/10.1016/J.GCA.2007.03.018.

Neff, U., Burns, S.J., Mangini, A., Mudelsee, M., Fleitmann, D., Matter, A., 2001. Strong coherence between solar variability and the monsoon in Oman between 9 and 6 kyr ago. Nature 411, 290–293. https://doi.org/10.1038/35077048.

Novello, V.F., Vuille, M., Cruz, F.W., Stríkis, N.M., de Paula, M.S., Edwards, R.L., Cheng, H., Karmann, I., Jaqueto, P.F., Trindade, R.I.F., Hartmann, G.A., Moquet, J.S., 2016. Centennial-scale solar forcing of the South American Monsoon System recorded in stalagmites. Sci. Rep. 6, 24762. https://doi.org/10.1038/srep24762.

Otto-Bliesner, B.L., Brady, E.C., Fasullo, J., Jahn, A., Landrum, L., Stevenson, S., Rosenbloom, N., Mai, A., Strand, G., Otto-Bliesner, B.L., Brady, E.C., Fasullo, J., Jahn, A., Landrum, L., Stevenson, S., Rosenbloom, N., Mai, A., Strand, G., 2016. Climate variability and change since 850 CE: an ensemble approach with the Community Earth System Model. Bull. Am. Meteorol. Soc. 97, 735–754. https://doi.org/10.1175/BAMS-D-14-00233.1.

PAGES Hyro2k Consortium, 2017. Comparing proxy and model estimates of hydroclimate variability and change over the Common Era. Clim. Past 13, 1851–1900. https://doi.org/10.5194/cp-13-1851-2017.

Pathak, A., Ghosh, S., Martinez, J.A., Dominguez, F., Kumar, P., Pathak, A., Ghosh, S., Martinez, J.A., Dominguez, F., Kumar, P., 2017. Role of oceanic and land moisture

sources and transport in the seasonal and interannual variability of summer monsoon in India. J. Clim. 30, 1839–1859. https://doi.org/10.1175/JCLI-D-16-0156.1.

Pausata, F.S.R., Battisti, D.S., Nisancioglu, K.H., Bitz, C.M., 2011. Chinese stalagmite δ^{18}O controlled by changes in the Indian monsoon during a simulated Heinrich event. Nat. Geosci. 4, 474–480. https://doi.org/10.1038/ngeo1169.

Richey, J.N., Sachs, J.P., 2016. Precipitation changes in the western tropical Pacific over the past millennium. Geology 44, 671–674. https://doi.org/10.1130/G37822.1.

Robock, A., 2000. Volcanic eruptions and climate. Rev. Geophys. 38, 191–219. https://doi.org/10.1029/1998RG000054.

Sachs, J.P., Sachse, D., Smittenberg, R.H., Zhang, Z., Battisti, D.S., Golubic, S., 2009. Southward movement of the Pacific intertropical convergence zone AD1400–1850. Nat. Geosci. 2, 519–525. https://doi.org/10.1038/ngeo554.

Sigl, M., McConnell, J.R., Toohey, M., Curran, M., Das, S.B., Edwards, R., Isaksson, E., Kawamura, K., Kipfstuhl, S., Krüger, K., Layman, L., Maselli, O.J., Motizuki, Y., Motoyama, H., Pasteris, D.R., Severi, M., 2014. Insights from Antarctica on volcanic forcing during the Common Era. Nat. Clim. Chang. 4, 693–697. https://doi.org/10.1038/nclimate2293.

Sinha, A., Berkelhammer, M., Stott, L., Mudelsee, M., Cheng, H., Biswas, J., 2011a. The leading mode of Indian Summer Monsoon precipitation variability during the last millennium. Geophys. Res. Lett. 38. https://doi.org/10.1029/2011GL047713.

Sinha, A., Cannariato, K.G., Stott, L.D., Cheng, H., Edwards, R.L., Yadava, M.G., Ramesh, R., Singh, I.B., 2007. A 900-year (600 to 1500 A.D.) record of the Indian summer monsoon precipitation from the core monsoon zone of India. Geophys. Res. Lett. 34. https://doi.org/10.1029/2007GL030431.

Sinha, A., Stott, L., Berkelhammer, M., Cheng, H., Edwards, R.L., Buckley, B., Aldenderfer, M., Mudelsee, M., 2011b. A global context for megadroughts in monsoon Asia during the past millennium. Quat. Sci. Rev. 30, 47–62. https://doi.org/10.1016/j.quascirev.2010.10.005.

Solanki, S.K., Usoskin, I.G., Kromer, B., Schüssler, M., Beer, J., 2004. Unusual activity of the Sun during recent decades compared to the previous 11,000 years. Nature 431, 1084–1087. https://doi.org/10.1038/nature02995.

Tan, L., Cai, Y., Cheng, H., Edwards, L.R., Lan, J., Zhang, H., Li, D., Ma, L., Zhao, P., Gao, Y., 2018. High resolution monsoon precipitation changes on southeastern Tibetan Plateau over the past 2300 years. Quat. Sci. Rev. 195, 122–132. https://doi.org/10.1016/J.QUASCIREV.2018.07.021.

Thirumalai, K., DiNezio, P.N., Okumura, Y., Deser, C., 2017. Extreme temperatures in Southeast Asia caused by El Niño and worsened by global warming. Nat. Commun. 8, 15531. https://doi.org/10.1038/ncomms15531.

Tierney, J.E., Oppo, D.W., Rosenthal, Y., Russell, J.M., Linsley, B.K., 2010. Coordinated hydrological regimes in the Indo-Pacific region during the past two millennia. Paleoceanography 25. https://doi.org/10.1029/2009PA001871.

Vieira, L.E.A., Solanki, S.K., Krivova, N.A., Usoskin, I., 2011. Evolution of the solar irradiance during the Holocene. Astron. Astrophys. 531, A6. https://doi.org/10.1051/0004-6361/201015843.

Wang, Y., Cheng, H., Edwards, R.L., He, Y., Kong, X., An, Z., Wu, J., Kelly, M.J., Dykoski, C.A., Li, X., 2005. The Holocene Asian monsoon: links to solar changes and North Atlantic climate. Science 308, 854–857. https://doi.org/10.1126/science.1106296.

Wang, Y.J., Cheng, H., Edwards, R.L., An, Z.S., Wu, J.Y., Shen, C.C., Dorale, J.A., 2001. A high-resolution absolute-dated late Pleistocene Monsoon record from Hulu Cave, China. Science 294, 2345–2348. https://doi.org/10.1126/science.1064618.

Wong, C.I., Breecker, D.O., 2015. Advancements in the use of speleothems as climate archives. Quat. Sci. Rev. 127, 1–18. https://doi.org/10.1016/J.QUASCIREV.2015.07.019.

Yamoah, K.A., Chabangborn, A., Chawchai, S., Schenk, F., Wohlfarth, B., Smittenberg, R.H., 2016. A 2000-year leaf wax-based hydrogen isotope record from Southeast Asia suggests low frequency ENSO-like teleconnections on a centennial timescale. Quat. Sci. Rev. 148, 44–53. https://doi.org/10.1016/j.quascirev.2016.07.002.

Yan, H., Sun, L., Oppo, D.W., Wang, Y., Liu, Z., Xie, Z., Liu, X., Cheng, W., 2011. South China Sea hydrological changes and Pacific Walker Circulation variations over the last millennium. Nat. Commun. 2, 293. https://doi.org/10.1038/ncomms1297.

Yan, H., Wei, W., Soon, W., An, Z., Zhou, W., Liu, Z., Wang, Y., Carter, R.M., 2015. Dynamics of the intertropical convergence zone over the western Pacific during the Little Ice Age. Nat. Geosci 8, 315–320.

Yang, H., Johnson, K.R., Griffiths, M.L., Yoshimura, K., 2016. Interannual controls on oxygen isotope variability in Asian monsoon precipitation and implications for paleoclimate reconstructions. J. Geophys. Res. Atmos. 121, 8410–8428. https://doi.org/10.1002/2015JD024683.

Yu, B., Zwiers, F.W., 2010. Changes in equatorial atmospheric zonal circulations in recent decades. Geophys. Res. Lett. 37, 5701. https://doi.org/10.1029/2009GL042071.

Zhang, H., Griffiths, M.L., Chiang, J.C.H., Kong, W., Wu, S., Atwood, A., Huang, J., Cheng, H., Ning, Y., Xie, S., 2018. East Asian hydroclimate modulated by the position of the westerlies during Termination I. Science 362, 580–583. https://doi.org/10.1126/science.aat9393.

Zhang, P., Cheng, H., Edwards, R.L., Chen, F., Wang, Y., Yang, X., Liu, J., Tan, M., Wang, X., Liu, J., An, C., Dai, Z., Zhou, J., Zhang, D., Jia, J., Jin, L., Johnson, K.R., 2008. A test of climate, sun, and culture relationships from an 1810-year Chinese cave record. Science 322, 940–942. https://doi.org/10.1126/science.1163965.

Zhao, K., Wang, Y., Edwards, R.L., Cheng, H., Liu, D., Kong, X., 2015. A high-resolved record of the Asian Summer Monsoon from Dongge Cave, China for the past 1200 years. Quat. Sci. Rev. 122, 250–257. https://doi.org/10.1016/j.quascirev.2015.05.030.